Biogeosciences Discussions

Biogeosciences Discussions is the access reviewed discussion forum of *Biogeosciences*

Simulating carbon and water cycles of larch forests in East Asia by the BIOME-BGC model with AsiaFlux data

M. Ueyama[1], K. Ichii[2], R. Hirata[3], K. Takagi[4], J. Asanuma[5], T. Machimura[6], Y. Nakai[7], T. Ohta[8], N. Saigusa[9], Y. Takahashi[9], and T. Hirano[10]

[1]Osaka Prefecture Univ., Graduate School of Life and Environmental Sciences, 1-1 Gakuen-cho, Naka-ku, Sakai, Osaka, Japan
[2]Fukushima Univ., Faculty of Symbiotic Systems Science, 1 Kanayagawa, Fukushima, Japan
[3]National Institute for Agro-Environmental Sciences, 3-1-1 Kannondai, Tsukuba, Ibaraki, Japan
[4]Hokkaido University, Field Science Center for Northern Biosphere, North 3-jo West 8-chome, Sapporo, Hokkadio, Japan

Title Page

Abstract | Introduction

Conclusions | References

Tables | Figures

◄◄ | ►►

◄ | ►

Back | Close

Full Screen / Esc

Printer-friendly Version

Interactive Discussion

[5] Univ. of Tsukuba, Graduate School of Life and Environmental Sciences, 1-1-1 Tennodai, Tsukuba, Ibaraki, Japan

[6] Osaka University, Graduate School of Engineering, 2-1 Yamadaoka, Suita, Osaka, Japan

[7] Forestry and Forest Products Research Institute, 1 Matsunosato, Tsukuba, Japan

[8] Nagoya Univ., Graduate School of Bioagricultural Sciences, Furo-cho, Chikusa Ward, Nagoya, Aichi, Japan

[9] National Institute for Environmental Studies, Center for Global Change Environmental Research, 16-2 Onogawa, Tsukuba, Ibaraki, Japan

[10] Hokkaido University, Research Faculty of Agriculture, Kita 9, Nishi 9, Kita-ku, Sapporo, Hokkadio, Japan

Simulating larch forests

M. Ueyama et al.

Abstract

Larch forests are widely distributed across many cool-temperate and boreal regions, and they are expected to play an important role in global carbon and water cycles. Model parameterizations for larch forests still contain large uncertainties owing to a lack of validation. In this study, a process-based terrestrial biosphere model, BIOME-BGC, was tested for larch forests at six AsiaFlux sites and used to identify important environmental factors that affect the carbon and water cycles at both temporal and spatial scales.

The model simulation performed with the default deciduous conifer parameters produced results that had large differences from the observed net ecosystem exchange (NEE), gross primary productivity (GPP), ecosystem respiration (RE), and evapotranspiration (ET). Therefore, we adjusted several model parameters in order to reproduce the observed rates of carbon and water cycle processes. This model calibration, performed using the AsiaFlux data, significantly improved the model performance. The simulated annual GPP, RE, NEE, and ET from the calibrated model were highly consistent with observed values.

The observed and simulated GPP and RE across the six sites are positively correlated with the annual mean air temperature and annual total precipitation. On the other hand, the simulated carbon budget is partly explained by the stand disturbance history in addition to the climate. The sensitivity study indicates that spring warming enhances the carbon sink, whereas summer warming decreases it across the larch forests. The summer radiation is the most important factor that controls the carbon fluxes in the temperate site, but the VPD and water conditions are the limiting factors in the boreal sites. One model parameter, the allocation ratio of carbon between aboveground and belowground, is site-specific, and it is negatively correlated with the annual climate of annual mean air temperature and total precipitation. Although this study significantly improves the model performance, the uncertainties that remain in terms of the sensitivity to water conditions should be examined in ongoing and long-term observations.

1 Introduction

The northern high latitude region is currently undergoing rapid and drastic warming (IPCC, 2007); the air temperatures in Eastern Siberia have risen by 7°C in winter and 1–2°C in annual during the past few decades (Dolman et al., 2008). The terrestrial
5 ecosystems in this region have responded to the warming climate through various feed-back processes (Chapin et al., 2005; Hinzman et al., 2005). These changes are likely to affect the carbon and water cycles in boreal and cool temperate forests, altering snow cover, permafrost dynamics, growing season length, and the severity of summer drought.
10   The predicted climatic changes affect the seasonal weather patterns differently (e.g. Manabe et al., 1992), and it is particularly important to understand how the changes in weather patterns affect terrestrial carbon and water cycles. The effects of current and future climatic changes on the terrestrial carbon and water cycles over northern high-latitude ecosystems are complex. Detected and/or potential effects include: (1) the
15 earlier onset of photosynthetic activity in high-latitude forests due to the spring warm-ing (Myneni et al., 2001; Kimball et al., 2004) leads to greater productivity and thus potentially increases the carbon sink (e.g. Keyser et al., 2000; Euskirchen et al., 2006; Welp et al., 2007); (2) the warming climate potentially stimulates the decomposition of soil carbon (Valentini et al., 2000; Piao et al., 2007; Ueyama et al., 2009) and reduces
20 carbon sink; and (3) atmospheric drying over the regions of warming could affect the carbon and water cycles of boreal forests since the carbon and water fluxes of boreal forests in Eurasia are highly sensitive to changes in atmospheric humidity (e.g. Schulze et al., 1999; Wang et al., 2005; Ohta et al., 2008).
     A number of terrestrial biosphere models have been applied to simulate the car-
25 bon and water cycles in high-latitude ecosystems (Euskirchen et al., 2006; Kimball et al., 2007). Although these models were tested with the data observed over the high-latitude biomes (Amthor et al., 2001; Grant et al., 2005), these validations were mostly conducted for evergreen conifer (Cienciala et al., 1998; Clein et al., 2002; Ueyama et

al., 2009), deciduous broadleaf (Kimball et al., 1997a), or arctic tundra ecosystems (Engstrom et al., 2006), but rarely conducted for the deciduous conifer (larch) forests. The lack of validation studies for larch forests could induce uncertainties in predicting the high-latitude and global carbon and water cycles.

5   Larch forests are widely distributed over many cool-temperate and boreal regions in the northern hemisphere (Gower and Richards, 1990). Across Eurasia to East Asia, a number of eddy covariance measurements have been conducted for several larch forests near the arctic (e.g. Ohta et al., 2001; Machimura et al., 2005; Nakai et al., 2008) and over boreal (Wang et al., 2005; Li et al., 2005) and cool temperate (Hirata

10 et al., 2007) regions. These measurements have revealed the important processes that determine the carbon and water cycles in larch forests, such as the environmental factors that control evapotranspiration (Ohta et al., 2008) and carbon flux (Hollinger et al., 1998; Wang et al., 2005; Li et al., 2005; Hirata et al., 2007; Nakai et al., 2008), and the role of stand disturbance (Machimura et al., 2007). Since these analyses are

15 site-specific, we need to analyze them at multiple site scales to clarify how the carbon and water fluxes spatially distribute, how the responses to the environmental conditions differ spatially, and how terrestrial biosphere models perform well. These studies are limited for larch forest ecosystems due to lack of enough observations, compared with the other forest ecosystems in North America (Baldocchi et al., 2001; Thornton et

20 al., 2002) and Europe (Valentini et al., 2000). However, the recent data accumulation makes it possible to conduct synthesis studies for this ecosystem.

    This study is a first step to understand the carbon and water cycle of larch forest in northern Eurasia to East Asia. In this study, a process-based terrestrial biosphere model, BIOME-BGC (Thornton et al., 2002), was tested for larch forests at six AsiaFlux

25 sites and used to identify important environmental factors that affect the carbon and water cycles at both temporal and spatial scales. Our specific objectives are to (1) improve the model performance by using the observed flux data; (2) clarify the environmental factors, including climate and stand disturbance, that control the carbon and water fluxes across the larch forests in East Asia; and (3) examine the response of the

carbon budget to changes in seasonal weather patterns.

2 AsiaFlux data

2.1 Site descriptions

The present study is a synthesis of 12 years of site data from six larch forests from Eurasia to East Asia (Fig. 1). The sites include the Tomakomai site (TMK), Japan; the Laoshan site (LSH), China; the Southern Khentii Taiga site (SKT), Mongolia; the Yakutsk site (YLF), Russia; the Neleger site (NEL), Russia; and the Tura site (TUR) in Russia. These sites are part of the AsiaFlux network (Hirata et al., 2008; Saigusa et al., 2008; Mizoguchi et al., 2009), covering a broad range of climate with annual precipitation totals from 240 mm to 1,750 mm per year and annual mean air temperatures from −10°C to 10°C. In terms of seasonal climatic variations (Fig. 2), TMK is characterized as a cool temperate climate with a cool early summer, warm winter and spring, and high humidity over the course of the year (low summer VPD and sufficient precipitation). The LSH and SKT sites are characterized by a boreal climate with cold winters, hot summers, dry atmospheric conditions, although LSH has much more precipitation during the summer than SKT. All of the Russian sites (YLF, NEL, and TUR) are characterized by a severe continental climate with cold winters, hot and dry summers, and low precipitation totals. Details of site information are summarized in Table 1.

TMK is a planted Japanese larch (*Larix kaempferi*) forest located at approximately 15 km northwest of Tomakomai, Hokkaido, in northern Japan (Hirano et al., 2003; Hirata et al., 2007). The stand was planted in 1957–1959, and the stand age was about 45 years old at the time of this study. The forest was sparsely dominated by broadleaf trees (*Betula ermanii*, *Betula platyphylla*, and *Uhnus japonica*) and spruce (*Picea jezoensis*) with understory of fern (*Dryopteris crassirhizoma* and *Dryopteris austriaca*). The maximum LAI of larch, other overstory species, and understory species were about 3.1, 2.5, and 3.6 $m^2 m^{-2}$ in summer, respectively.

LSH is a planted larch (*Larix gmelinii*) forest in northern China (Wang et al., 2005a,b). The forest was established as a plantation in 1969 as a pure larch forest. The maximum LAI of larch trees was about $2.5\,m^2\,m^{-2}$. Some broadleaf species sparsely consisted of the canopy (e.g. *Betula platyphylla*, and *Fraxinus mandshurica*). The forest floor was covered by the understory vegetations, such as some shrub species, and *Cyperaceous* and *Liliaceous* families.

SKT is a Siberian larch (*Larix sibirica*) forest located at approximately 25 km northeast of the Mongonmorit village in the Tov province of Mongolia (Li et al., 2005, 2006, 2007). The age structure of the larch range from ~70 to over 150 years old, but the oldest trees are older than 300 years. The forest experienced a large-scale fire in 1996–1997 in which approximately 37.5% of the total stem density was burnt. The understory was formed distinct layer of grass and scattered shrubs. The maximum LAI of the larch and understory species were about 2.7 and $1.7\,m^2\,m^{-2}$, respectively.

YLF is a Cajander larch (*Larix cajanderi*) forest located approximately 20 km north of Yakutsk, Russia, eastern Siberia (Ohta et al., 2001, 2008; Dolman et al., 2004). The larch are on permafrost soil with an active layer depth of approximately 1.2 m. The LAI of the larch needles was $1.56\,m^2\,m^{-2}$, whereas the forest floor was covered by a dense understory of vegetation, such as *Vaccinium* families, with an LAI of $2.1\,m^2\,m^{-2}$. Since there has not been a fire at the site for at least the last 80 years, the average stand age is 160 years.

NEL is a larch (*Larix cajanderi*) forest located on the approximately 30 km northwest of Yakutsk, Russia (Machimura et al., 2005, 2007). The forest is also on continuous permafrost with an active layer depth of approximately 1.0 m. The average stand height was 8.6 m, and the maximum tree height was approximately 21 m. The forest floor was covered by *Vaccinium uliginosum* and *Pyrola incarnate* with moss species. The LAI of the larch needle was $1.9\,m^2\,m^{-2}$, whereas that of the understory was $1.0\,m^2\,m^{-2}$.

TUR is a Gmelin larch (*Larix gmelinii*) forest located in Tura in the Evenkia Autonomous District in Central Siberia (Nakai et al., 2008). The stand age is about 105 years old. The LAI of the larch needles was ~$0.3\,m^2\,m^{-2}$. The soil type is Cryosol, and

the permafrost table is within a 1 m depth. The forest floor was covered by some shrub species, such as *Betula nana*, *Ledum palustre*, *Vaccinium uliginosum*, and *Vaccinium vitis-idaea*. The ground was densely covered with lichens and mosses.

2.2 Data processing

We used the observed carbon and water fluxes from the eddy covariance method for the six tower-sites. The observed net ecosystem exchange (NEE) were partitioned into ecosystem respiration (RE) and gross primary productivity (GPP) using relationships obtained from the nighttime NEE and air temperature (Hirata et al., 2008; Takagi et al., personal communication, 2009). Quality control and gap-fill of the data were conducted by standardized methods (Hirata et al., 2008; Takagi et al., personal communication, 2009). Observed half-hourly fluxes and meteorology were aggregated to a daily basis for the model input. In this study, negative and positive NEE values indicate a net sink and source of atmospheric carbon, respectively.

3 Model

3.1 BIOME-BGC model

The carbon and water cycles of the larch forests were simulated using the BIOME-BGC model (Thornton et al., 2002). The BIOME-BGC is a process-based terrestrial ecosystem model that simulates biogeochemical and hydrologic processes across multiple biomes. The model is driven at a daily time scale with the meteorological values of the daily maximum, minimum, and average air temperatures, precipitation, daytime VPD, and solar radiation.

Evapotranspiration (ET) is estimated from the sum of transpiration, evaporation from the soil and canopy, and sublimation (Kimball et al., 1997b). Evapotranspiration is basically calculated by a Penman-Monteith model (Running and Coughlan, 1988). Soil conductance is simply estimated from the number of days since a rainfall event. Canopy

Simulating larch forests

M. Ueyama et al.

|◀ | ▶|

◀ | ▶

Back | Close

Full Screen / Esc

evaporation is estimated from the amount of water intercepted by the canopy. Transpiration is regulated by the canopy conductance under the daily meteorological conditions of the minimum air temperature, VPD, solar radiation, and soil water condition (Jarvis, 1978).

5   The model has three compartments for carbon and nitrogen: vegetation, litter, and soil. Each compartment is subdivided into four pools on the basis of differences in their function (e.g., leaf, stems, course roots, and fine roots) and residence time (e.g., active, intermediate, slow, and passive recycling). GPP is estimated by combing the Farquhar biochemical model (Farquhar et al., 1980) with the stomatal conductance model
10 (Jarvis, 1978). Ecosystem respiration (RE) is calculated as the sum of autotrophic and heterotrophic respiration (AR and HR). The AR and HR are calculated from the carbon and nitrogen pools and the temperature (for AR and HR) and soil water condition (for HR only). Further details for the BIOME-BGC model have been described in previous papers (e.g., Kimball et al., 1997a,b; Thornton et al., 2002; Ueyama et al., 2009).

15 **3.2   Model modifications**

To improve the model performance for the larch forests, we applied three modifications to the original model. The requirement of these modifications were found by checking the default model output with field observations such as carbon and water cycles, seasonal variation in snow cover, and soil temperature. First, we incorporated the
20 seasonality of the percent of leaf nitrogen in Rubisco (PLNR) based on the strong seasonal variation in the leaf C:N ratio in larch trees (Kim et al., 2005) and the seasonality of PLNR in deciduous trees (Wilson et al., 2000) as follows:

$$
\begin{aligned}
&\text{PLNR}(d) = \text{PLNR}_{\text{base}} && (d < 200) \\
&\text{PLNR}(d) = \text{PLNR}_{\text{base}}\sqrt{\dfrac{\text{CN}_{\text{leaf}}}{\text{CN}_{\text{litter}} - (\text{CN}_{\text{litter}} - \text{CN}_{\text{leaf}}) * S}} && (d \geq 200) \\
&S = \sin\left(\dfrac{d - (d_{\text{onset}} + 1)}{d_{\text{growth}} + 1}\pi\right)
\end{aligned}
\tag{1}
$$

where PLNR$_{base}$ is the maximum PLNR (which corresponds to the PLNR of the original BIOME-BGC model); CN$_{leaf}$ is the leaf C:N ratio; CN$_{litter}$ is the litter C:N ratio; d is the day of the year; d$_{onset}$ is the onset day; and d$_{growth}$ is the length of the growing period. The incorporation of this seasonality produces a higher GPP in the beginning of the growing season and then a gradual declines of GPP during the latter growing season, results which are consistent with flux tower-based GPP measurements (Hirata et al., 2007).

Second, the original BIOME-BGC model significantly overestimated the snow sublimation, which induced an unreasonable snow disappearance in late winter and thus a water deficit in the boreal summer and autumn. We simply modeled the snow disappearance by using only daily the air temperature in order to make the model reproduce the observed variations of water and carbon fluxes.

Third, we used the monthly moving average for the estimation of soil temperature for further reproduction of the observed results, although the original BIOME-BGC model estimated the soil temperature by using the 10-day moving average of the daily air temperature. The estimated soil temperature during the snow period was also overestimated in the TMK site by the original BIOME-BGC model; this was probably caused by the overestimation of the snow insulation effect. We changed the parameter for the insulation effect from 0.83 to 0.55 at the simulations of TMK to reproduce the observed soil temperature. This calibration decreased the soil temperature during the snow period and thus decreased the root respiration and HR in the winter.

3.3 Model initializations

The model was initialized by a spinup run, in which the dynamic equilibriums of the soil organic matter and vegetation components were determined by using a constant CO$_2$ concentration of 296 ppm and the observed daily meteorological data and ecophysiological parameters (Table 2). We used soil texture data (Zobler, 1986) and rooting depth data (Webb et al., 1993) as the model inputs for the sites where site-specific observation is not available. Only for the YLF, NEL and TUR sites, we used the ob-

Simulating larch forests

M. Ueyama et al.

served seasonal maximum of the active layer depth as effective rooting depth. Using the spinup-endpoint as an initial condition, we conducted the model simulations from 1915 to the final year of the observations with the ambient CO_2 concentration (Enting et al., 1994; Tans and Conway, 2005). In these simulations, we repeatedly used the observed meteorology at the site rather than the long-term meteorological records from the weather stations near the sites in order to avoid biases due to data discontinuities. Since the observations at YLF, NEL, and TUR were only conducted during periods of the vegetation growth, we used the meteorological data of the National Climate Data Center (NCDC) from weather stations near the sites for the model input for those winter periods.

We implemented simple disturbance treatments for TMK and LSH as plantation and SKT as fire based on the definitions presented by Thornton et al. (2002). For the plantation disturbance of TMK and LSH, we assumed that the amount of vegetation planted was 30% of the dynamic equilibrium of the vegetation, and the rest was removed from the sites; the leaf and fine root C and N pools were included in the fine litter pool. The aboveground live and dead wood C and N pools were removed from the site, and the belowground live and dead wood C and N pools were included in the course woody debris (CWD) pools (Thornton et al., 2002). Based on the stand history (Hirano et al., 2003; Wang et al., 2005a), we assumed that the plantations were established in 1959 for TMK and in 1969 for LSH. Since the stands experienced a large-scale fire in 1996 and 1997 at SKT (Li et al., 2005), we also implemented a fire disturbance in which 37.5% of the forest was affected. The proportions of the leaf, fine root, live wood, and fine litter C and N pools were assumed to be consumed in the fire and lost to the atmosphere, and the affected portions of the dead wood C and N pools were sent to the CWD pools (Thornton et al., 2002). Although the stand disturbance history of the mature forest sites in YLF, NEL, and TUR were not available, we inserted a fire disturbance just after the spinup run (year of 1915) for YLF, NEL, and TUR, assuming that the same amount as in SKT, 37.5%, was affected by the ground fire based on the fact that Siberian larch forests experience a ground fire every 20–50 years (Schulze et al.,

[BGD](#)

6, 8311–8357, 2009

Simulating larch forests

M. Ueyama et al.

Title Page

Abstract | Introduction

Conclusions | References

Tables | Figures

◄ | ►

◄ | ►

Back | Close

Full Screen / Esc

Printer-friendly Version

Interactive Discussion

Simulating larch forests

M. Ueyama et al.

1999).

3.4 Model applications

We first simulated the carbon and water fluxes by using the original BIOME-BGC model with the original parameters for deciduous needle leaf forest (DNF) shown in Table 2 (White et al., 2000). Then, we calibrated the modified model by using the AsiaFlux data observed at the six larch forests, and evaluated how the AsiaFlux data could improve the model performance for the larch forests in East Asia. Most of the default ecophysiological parameters for DNF are from those for evergreen needleleaf forest (White et al., 2000) owing to limitation of data availability. We updated the new general parameters for DNF in Table 2, referring the literature available data; all of parameters were common across the six sites except for the two site-specific parameters. The model was parameterized according to the following criteria: (1) the parameters were at first changed at a minimum in order to reduce biases in the fluxes, such as the magnitude of day-to-day variations and unrealistic declines due to suppression effects, by referring to the previous studies; and (2) the peak of GPP was adjusted by changing the allocation ratio between new fine roots C to new leaf C (A_{root_leaf}). Assuming that the allocation ratio between aboveground and belowground components strongly depends on the climatic conditions (e.g., Friedlingstein et al., 1999; Chapin et al., 2002; Vogel et al., 2008), the parameter for A_{root_leaf} was determined for each site. The canopy interception coefficient in LSH was only changed to 0.005 LAI^{-1} d^{-1} in order to reproduce the observed ET. In both the original and the improved simulation, we applied the stand disturbance treatment in the model initialization (as described in Sect. 3.3). To understand the role of stand disturbance on the annual carbon budget, the observed annual carbon budgets were also compared to the simulated results with and without the stand disturbances.

Next, the spatial distributions of the modeled carbon fluxes were examined by using the annual climatology of each site. The simulated annual values of carbon fluxes from the improved model were compared with the annual climatology of air temperature,

precipitation, and radiation to clarify the important climatic variables for determining the spatial variations in the fluxes.

Then, to understand the response of the carbon cycle to changes in the weather conditions, we conducted a sensitivity analysis with biased meteorological data, by giving either warmer or cooler, wetter or dryer, and sunnier or cloudier biases for each season; winter (December to February), spring (March to May), summer (June to August), and autumn (September to November). The biases were determined as 3σ (σ is the standard deviation) of the long-term natural climate variabilities (Table 3). The natural climate variabilities for air temperature, precipitation, and VPD in TMK were estimated by using the weather station data observed by the Japan Meteorological Agency (JMA) from 1961 to 2000, whereas those in LSH, SKT, YLF, NEL, and TUR were estimated from the observations that were made from 1961 to 2000 by the NCDC. The variabilities for radiation were derived from the International Satellite Cloud Climatology Project Radiation Flux Profile data from 1984 to 2000 (ISCCP-FD; Zhang et al., 2004) centered on the observed site.

4 Results and discussions

4.1 Model validation

The original model generally underestimated carbon flux variations at daily, monthly, and annual time scales (Figs. 3, 5 and 6). At the daily time scale, the results were not perfectly consistent with the observed fluxes. They showed considerable scatter and underestimated or overestimated the observed values in each site (Fig. 3). The slopes between the observations and the simulation results were 0.65 for NEE, 0.73 for GPP, 0.60 for RE, and 0.70 for ET, which all deviated significantly from 1.0. The monthly variations of the simulated and observed fluxes also showed that the amplitude of the flux variation simulated by the original model was inconsistent with the observed results (Fig. 5). The peaks of GPP and RE were generally underestimated for TMK, SKT, and

BGD

6, 8311–8357, 2009

Simulating larch forests

M. Ueyama et al.

Title Page

Abstract	Introduction
Conclusions	References
Tables	Figures

Back | Close

Full Screen / Esc

Printer-friendly Version

Interactive Discussion

YLF and overestimated for NEL and TUR, although the seasonality, such as the onset and offset of the growing season, was generally reproduced. The annual GPP, RE, and ET were underestimated in TMK, but overestimated in other sites, resulting in slopes of regression lines that deviated from 1.0 (Fig. 6).

Using the observed fluxes as calibration data, the improved model successfully simulated the carbon and water fluxes at daily, monthly, and annual time scales (Figs. 4, 5 and 6). The seasonality of the carbon fluxes was also significantly improved (Fig. 5). Although the observed peak of GPP and NEE in the TMK site in June could not be reproduced by the original model, the improved model successfully reproduced the phase and amplitude of the carbon fluxes owing to the incorporation of the seasonality of PLNR, which was consistent with the observed results at the leaf (Kim et al., 2005) and canopy scales (Hirata et al., 2007). This improvement suggested that using a constant nitrogen ratio in the leaf could contribute to the uncertainty in the original BIOME-BGC model. In the boreal sites of YLF, NEL, and TUR, since the snow sublimation was reduced due to the modification, the water conserved during the winter were used in the summer periods in the improved model and thus mitigated the water stress (Fig. 5d), resulting in the improvement in an seasonality of ET for YLF. Although the carbon fluxes were significantly improved in the model, the simulated ET at the daily time scale was not significantly improved, compared with the carbon fluxes. This discrepancy might be caused by both the observation and simulation (shown in Sect. 4.4).

The improvements of the model reduced the root mean square error (RMSE) at almost every site (Table 4). The results from the improved model simulation highly correlated with the observed GPP (R^2=0.99), RE (R^2=0.98), and ET (R^2=0.86), compared to the results from the original simulation (Fig. 6). The annual carbon budget simulated by the model was also improved by the calibrations. On the other hand, the improved model still only explained 41% of the variation in the observed carbon budget (Fig. 6a); the simulated results by the improved model had a tendency to underestimate the observed carbon uptake.

Simulating larch forests

M. Ueyama et al.

Title Page

Abstract | Introduction

Conclusions | References

Tables | Figures

⏮ | ⏭

◀ | ▶

Back | Close

Full Screen / Esc

Printer-friendly Version

Interactive Discussion

The inclusion of the stand history is an important factor for improving annual NEE estimation (Fig. 7). If we run the model without including stand history, the simulated NEE was significantly underestimated in both the original and improved models. The simulations run without including the stand history could not reproduce the observed annual NEE (R^2=0.13), whereas those considering the stand history reproduce 50% of the variation. The model performance for estimation of the annual NEE was improved by considering the stand history; the annual sink was increased in the planted sites of TMK and LSH and the fire-disturbed site of SKT by considering the stand histories.

Overall, the model was successfully improved by the calibration with regional network of flux tower measurements. The improved model reasonably reproduced the carbon and water fluxes at the daily, monthly, and annual time scales. Therefore, the improved model allowed us to evaluate the spatial distributions of the fluxes and the sensitivity of the fluxes to the weather conditions.

4.2 Spatial gradient of carbon cycle and climate

The responses of the simulated annual carbon and water fluxes to the annual climate were shown in Fig. 8. Across the six sites, the simulated GPP and RE significantly increased with the annual air temperature (R^2=0.84; p <0.01 for GPP and R^2=0.82; p <0.01 for RE) as well as the annual precipitation (R^2=0.86; p <0.01 for GPP and R^2=0.85; p <0.01 for RE), and there was no clear relationship between those fluxes and the amount of radiation (R^2=0.20; p=0.38 for GPP and R^2=0.16; p=0.38 for RE). Since there was a strong correlation between annual air temperature and precipitation across the sites, we could not identify which of these processes was a more important controlling factor for explaining the spatial variation of those fluxes. Since the simulated annual fluxes were consistent with the observed results (Fig. 6), these trends were also applicable to the observed fluxes. Our results indicated that the air temperature and/or precipitation are potentially important controlling factors for explaining the spatial distribution of the carbon and water fluxes of larch forests.

Simulating larch forests

M. Ueyama et al.

Back | Close

Full Screen / Esc

Printer-friendly Version

Interactive Discussion

The simulated NEE was weakly correlated with the annual climate (Fig. 8) in that the annual carbon sink increased with an increase of the annual mean air temperature (R^2=0.55; p=0.09), precipitation (R^2=0.46; p=0.14), and radiation (R^2=0.50; p=0.12). Based on the correlation coefficients between NEE and the climate variables, the an-

5 nual mean air temperature was most strongly related to the spatial distribution of NEE. Although both the GPP and RE had positive correlations with the climate variables, a greater GPP induced a greater annual carbon sink, whereas a greater RE did not reduce this sink. This result suggested that the spatial distribution of NEE was generally determined by that of GPP rather than RE. Since the annual carbon budget was highly

10 sensitive to the stand history (Fig. 7), the spatial distribution of NEE was determined by both climate variables and stand disturbance history.

In the model calibration, we adjusted the seasonality of the fluxes by changing the parameter for the allocation ratio of carbon between aboveground and belowground (A_{root_leaf}). The obtained site-specific A_{root_leaf} showed a week negative correlation with

15 the mean annual air temperature (R^2=0.24; p=0.30) and total precipitation (R^2=0.24; p=0.18) (Fig. 9). These trends were statistically significant (R^2=0.91; p=0.02 for air temperature, R^2=0.77; p=0.05 for total precipitation) when the relationships were obtained by eliminating LSH (dashed lines in Fig. 9), since the carbon fluxes of LSH might be affected by tree species other than larch due to the limited footprint (H. Wang,

20 personal communication, 2008). The negative trends indicate that the forests could allocate more carbon aboveground under warmer and wetter climate, but belowground under colder and dryer climate. The obtained trend of A_{root_leaf} can be explained by the allocation strategy of plants that adjust resource acquisition to maximize the capture of the most limiting factor (Chapin et al., 2002); light could be the most limiting factor

25 under a favorable climate, whereas soil water might limit net primary productivity (NPP) under a cold and dry environment. A similar result was reported by Vogel et al. (2008), who summarized the carbon allocation in boreal black spruce forests across North America; soil temperature positively correlated with the aboveground NPP and negatively correlated with the belowground NPP across those sites. The higher allocation to

Simulating larch forests

M. Ueyama et al.

belowground at northern sites is also consistent with the field survey of root system at TUR. Kajimoto et al. (2003) observed the greater rooting area of the larch trees compared with the crown projected area, and concluded that the larch trees on permafrost soil competed belowground resource rather than light environment. The simulated LAI was negatively correlated with the A_{root_leaf} (R^2=0.83) (Fig. 9), suggesting that A_{root_leaf} strongly constrained the LAI in the model simulation. The climatic conditions could strongly control the allocation strategy (Fig. 9a,b) and thus control the carbon fluxes (Fig. 8) through changing in the LAI (Fig. 9c). The strong correlation between A_{root_leaf} and the simulated LAI indicates that the satellite-derived LAI might be useful to infer the spatial distributions of A_{root_leaf} and improve the regional model simulation. This allocation parameter might also be inferred from the climate data in the regional simulations. Such a dynamic allocation scheme has been incorporated in some biosphere models (e.g. Friedlingstein et al. 1999; Sitch et al., 2003) and will improve the performance of the future projections made with the BIOME-BGC model.

4.3 Effect of seasonal climate anomalies on the carbon cycle

To understand the responses of carbon cycle to the weather conditions of air temperature, precipitation, VPD, and solar radiation, we examined the sensitivity of the larch forests to changes in the seasonal weather patterns (Sect. 3.4). The results of the sensitivity analysis were shown in Table 5.

Spring warming enhanced the carbon sink (Table 5 case ta), but the summer and autumn warming tended to decrease the sink (Table 5 case tc, and te). The spring warming enhanced GPP rather than RE except at SKT, where it resulted in the increase of the annual carbon sink (Table 5 case ta). This was because the spring warming induced the earlier onset of leaf emergence and enhanced photosynthetic activity, whereas RE was well regulated by the low soil temperature. On the other hand, summer, autumn, or winter warming decreased the annual carbon sink, except in the autumn of NEL, because the warming stimulated RE more than GPP (Table case 5tc–th). These results were consistent with the tower observations at TMK (Hirata et

al., 2007), SKT (Li et al., 2005), and another Siberian site (Hollinger et al., 1998). Tree-ring data for the Siberian larch also showed that these larch trees did not benefit from mid-summer to autumn warming (Vaganov et al., 1999; Kirdyanov et al., 2003). These results suggest that the future carbon budget of larch forests is dependent on the delicate changes in warming during the spring, summer, and autumn periods.

A change in precipitation significantly affected GPP and RE in SKT (Table 5 case pc and pd) in that a wetter summer enhanced both GPP and RE by mitigating the water stress to photosynthesis and decomposition. For other sites, a change in precipitation did not significantly influence GPP and RE, but it greatly influenced NEE, especially for the boreal sites of YLF, NEL, and TUR. Considering the low sensitivities of GPP and RE to precipitation, the high sensitivity of NEE might be exaggerated by small errors because NEE was the small difference of these two large terms. The forests of TMK and LSH did not respond strongly to the change in precipitation (Table case 5pa-ph), a result which was consistent with the observed studies (Hirata et al., 2007).

The sensitivity of the annual carbon budget to the change in VPD was only obvious in the boreal summer (Table 5 case vc and vd). The higher VPD in the summer regulated GPP and thus decreased the annual sinks of the LSH, SKT, YLF, and TUR sites (Table 5 case vc). On the other hand, the lower VPD in the summer mitigated the regulation of photosynthesis at SKT, resulting in the increase of the annual sink there (Table case 5 vd). This sensitivity to VPD was consistent with the observed results for LSH (Wang et al., 2005b), SKT (Li et al., 2005), and TUR (Nakai et al., 2008) as well as a comparative study between the TMK and LSH sites (Wang et al., 2005b). The reason for the low sensitivity to VPD at the TMK site is that the summer VPD is not high enough to sufficiently reduce the stomatal conductance (Fig. 2).

The GPP in the TMK site was the most sensitive to the change in solar radiation. An increase of approximately 12% of the annual GPP resulted in an approximately 70% enhancement of the annual carbon sink, compared to the control simulation (Table 5 case sc). The decline of summer radiation greatly decreased GPP and the magnitude of negative NEE, meaning a decrease in the annual sink at the TMK site (Table 5 case

[BGD](#)

6, 8311–8357, 2009

Simulating larch forests

M. Ueyama et al.

Title Page

Abstract | Introduction

Conclusions | References

Tables | Figures

◄ | ►

◄ | ►

Back | Close

Full Screen / Esc

Printer-friendly Version

Interactive Discussion

sd). Among the boreal sites of LSH, SKT, YLF, NEL, and TUR, the change in the radiation did not significantly affect the GPP regardless of the season, but the annual carbon sink (negative NEE) was positively correlated with the change in summer radiation. This higher sensitivity to radiation was also reported for the observed results at
5 TMK (Hirata et al., 2007). Considering the sensitivity to VPD, the summer VPD could be an important factor that controls the variations of the carbon budget, but the summer radiation might become an important factor if the regulation by VPD is not obvious.

The sensitivity studies showed what the important weather conditions were that control the annual carbon cycle in each site. In the temperate site of TMK, the change
10 in the summer radiation was simulated to be the most important factor for determining the annual carbon budget. On the other hand, the change in summer VPD most significantly affected the annual carbon budgets of the boreal sites of LSH, SKT, and YLF. The change in air temperature was also an important controlling factor of the annual carbon budgets among all the larch forests; a warmer spring could enhance the
15 carbon sink, but a warmer summer and autumn could decrease the sink. This temperature sensitivity was simulated to be the most important controlling factor of the carbon budget for the TUR and NEL sites.

4.4 Further model improvements and potential limitations

This study is a first attempt to validate a terrestrial biosphere model at multiple larch
20 forests sites in northern Eurasia to East Asia, showing several uncertainties of the default model. Our analysis demonstrated that the calibration by the AsiaFlux observations greatly improved the BIOME-BGC model at daily, monthly, and annual time scales, and the improved model enabled us to perform more accurate sensitivity studies. However, we should note the following limitations and potential improvements.
25 The simulated ET was still inconsistent with the observed ET at a daily time scale (Fig. 2). This disagreement was mainly caused by the intercepted evaporation term; the simulated intercepted evaporation was significantly large during the rainy days, whereas the observed ET was not too large. Considering that the eddy covariance

Simulating larch forests

M. Ueyama et al.

method could not perfectly measure ET during and just after rainfall (e.g. Kosugi et al., 2007), we could not validate the simulated intercepted evaporation. Ohta et al. (2001) reported that the intercepted evaporation was about 15% of the precipitation at the YLF site, a result which was consistent with the simulated intercepted evaporation value of
5 about 18% of the precipitation. Observed ET by the eddy covariance measurements also has uncertainties due to the energy imbalance problem (Wilson et al., 2002). The energy balance ratio at our study sites was ranged from 66% to 100% (Hirata et al., 2005; Liu et al., 2005; Wang et al., 2005; Nakai et al., 2008; Ohta et al., 2008), inducing significant uncertainties in observed ET and potentially in the carbon fluxes.
10 Although the simulated sensitivities to air temperature, VPD and radiation were consistent with the observed studies, the simulated response to precipitation still had large uncertainties. At the sites of TMK and LSH, the amount of precipitation did not significantly affect the modeled carbon budget; this was consistent with observations. On the other hand, the change in precipitation significantly affected the carbon budgets in the
15 northern sites of SKT, YLF, NEL, and TUR. Although the discrepancy in NEE might be exaggerated by small errors of the two large terms, the errors were partly caused by a lack of important processes in the model, such as the water supply from the deeper layer that the larch trees used when the water supply in the upper soil layer was limited (Li et al., 2006). Studies at YLF (Ohta et al., 2008) and NEL (Machimura et al., 2007)
20 showed a 1-year lag of the carbon and water fluxes to precipitation probably due to the availability of water stored in the permafrost. Consequently, further improvements of the model could be required to simulate the response to water conditions. Other factors that might contribute to the discrepancy could be due to the understory vegetation and/or permafrost dynamics (Ueyama et al., 2009).
25 The BIOME-BGC model considers only tree species in ecosystem, but larch stands generally consist of sparse canopy, coexisting with other species. Our study sites also contain trees and understory vegetations other than larch (shown in Sect. 2.1), the result which induced uncertainties in the model simulation.

Our simulation showed that the stand history was the most important factor for pre-

Simulating larch forests

M. Ueyama et al.

Printer-friendly Version

Interactive Discussion

dicting the carbon budget (Fig. 7). Although the spatial distribution of NEE was also highly sensitive to the climate variables (Fig. 8), the observed large carbon sink of TMK and SKT could not be reproduced without the stand history. These results suggest that the availability of information on stand history could improve the carbon budget simula-
5 tion both at stand (the YLF, NEL, and TUR sites, where stand history was not available) and regional scales.

Several model assimilation studies pointed out the problem of model equifinality in that many different model parameterizations are able to reproduce the observed data acceptably well (e.g. Franks et al., 1997; Schulz et al., 2001). To minimize the problem
10 of the model equifinality, we (1) modified the submodels by carefully checking the default model output with field observations other than the carbon and water fluxes, (2) examined the high sensitive parameters across the multiple sites through the sensitivity analysis, and (3) updated the parameters mainly from literature available values. In addition to the validation of current status of the fluxes, we also validated the ecosystem
15 sensitivity to the seasonal weather anomalies, and obtained a reasonable sensitivity compared with the observed studies in each site. Consequently, the examined parameters are likely minimized for the model equifinality, and are applicable to simulate the current status of larch forests of the multiple sites. While the model is well validated in this study, further data acquisition will improve the model parameterizations.
20 In this study, we initialized the model with the short-term meteorology at the tower sites rather than the long-term meteorological records from the weather stations near the sites, in order to avoid biases due to data discontinuities. This initialization might lead to some biases in the simulation. Since the historical changes in the climate affect the carbon and water cycles through various indirect feedbacks, such as changes in
25 the pool size (Keyser et al., 2000; Ueyama et al., 2009), the use of short-term meteorology might ignore these effects and lead to simulations that were more indicative of the steady state condition compared with the actual carbon and water cycles. The underestimation of the annual carbon sink by the model simulation (Fig. 6) might also be caused by this initialization process. Since the simulated sensitivity to the seasonal

weather conditions (Table 5) has been conducted for a short-term change (interannual time scale), the response of the carbon and water cycles to the long-term climate anomalies (e.g. decadal or longer time scales) should be examined in future studies.

5 Conclusions

The regional network of tower flux measurements, AsiaFlux, improved the model performance of the BIOME-BGC for larch forests in East Asia. Using the flux data at six sites from Siberian subarctic to cool temperate regions, we determined new general parameters for larch forests. The use of these validated parameters will allow us to apply at regional scale simulation. The site-specific parameter of the allocation ratio of new fine root C to new leaf C was negatively correlated with the annual climatology of air temperature and precipitation; this strongly constrained the simulated LAI. In the regional scale simulation, the allocation parameter will be estimated from the climate data or satellite derived LAI.

The model simulations showed that the spatial variations of GPP and RE were correlated with the variations in the annual climatology of air temperature and/or precipitation. In addition to the climatic conditions, the stand history was another important factor for explaining the spatial variations of NEE. These simulation results suggest that the spatial map of the disturbance history, such as plantation areas and fire, will be important for the projection of the regional scale carbon budget. For the future projections of the carbon cycle, the BIOME-BGC model will necessarily be coupled with a sophisticated disturbance algorithm at the regional to continental scale.

The sensitivity analysis showed that spring warming could enhance the carbon sink, but summer and autumn warming could decrease the carbon sink; this was consistent with the observed results. In one temperate site, where water conditions did not regulate the carbon cycle, summer radiation was the most important factor that controlled the annual carbon budget. On the other hand, summer VPD strongly regulated the annual carbon sink in the boreal sites. Since the sensitivity analysis has been conducted

for the seasonal to interannual time scale, it is not clear how long-term changes in climate affect the carbon and water cycles including various feedback processes. These projections should be examined in ongoing and long-term observations.

When comparing the observed data, the model uncertainties have been addressed in this study, especially for boreal regions. It is possible that the modeled response to the water conditions is inaccurate. In some boreal sites, the regulation of stomatal conductance and heterotrophic respiration by the water deficit might be overestimated. These discrepancies could be due to various causes, such as water storage in deeper soil layers, the effects of understory vegetation, and permafrost dynamics. Additional validation with available chamber and biometric measurements will reduce the model uncertainties.

This study is a first step to synthesize AsiaFlux data with modeling studies, demonstrating that 1) uncertainties of the biosphere model could be reduced with the flux data, and 2) the use of the validated model could improve our understanding of carbon and water fluxes at both temporal and spatial scales. In the future, we will conduct the synthesis studies with various biosphere models for various ecosystems in East Asia, along with regional scale simulations.

References

Amthor, J. S., Chen, J. M., Clein, J. S., Frolking, S. E., Goulden, M. L. Grant, R. F., Kimball, J. S., King, J. S., McGuire, A. D., Nikolov, N. T., Potter, C. S., Wang, S., and Wofsy, S. C.: Boreal forest CO_2 exchange and evapotranspiration predicted by nine ecosystem process models: Intermodel comparisons and relationships to field measurements, J. Geophys. Res., 106, 33623–33648, 2001.

Simulating larch forests

M. Ueyama et al.

⏮ | ⏭

◀ | ▶

Back | Close

Full Screen / Esc

Printer-friendly Version

Interactive Discussion

Baldocchi, D. D., Falge, E., Gu, L., Olson, R., Hollinger, D., Running, S., Anthoni, P., Nernhofer, C., Davis, K., Evans, R., Fuentes, J., Goldstein, A., Katul, G., Law, B., Lee, X., Malhi, Y., Meyers, T., Munger, W., Oechel, W., Paw U, K. T., Pilegaard, K., Schmid, H. P., Valentini, R., Verma, S., Vesala, T., Wilson, K., and Wofsy, S.: FLUXNET: A new tool to study the temporal and spatial variability of ecosystem-scale carbon dioxide, water vapor, and energy flux densities, B. Am. Meteorol. Soc., 82, 2415–2434, 2001.

Chapin III, F. S., Matson, P. A., and Mooney, H. A.: Principles of terrestrial ecosystem ecology, Springer-Verlag Press, New York, USA, 436 pp., 2002.

Chapin III, F. S., Sturm, M., Serreze, M. C., McFadden, J. P., Key, J. R. Lloyd, A. H. McGuire, A. D., Rupp, T. S., Lynch, A. H., Schimel, J. P., Beringer, W. L. Chapman, W. L., Epstein, H. E., Euskirchen, E. S., Hinzman, L. D., Jia, G., Ping, C. L., Tape, K. D., Thompson, C. D. C., Walker, D. A., and Welker, J. M.: Role of land-surface changes in arctic summer warming, Science, 310, 657–660, 2005.

Cienciala, E., Running, S. W., Lindroth, A., Grelle, A., and Ryan, M. G.; Analysis of carbon and water fluxes from the NOPEX boreal forest: comparison of measurements with FOREST-BGC simulations, J. Hydrol., 212–213, 62–78, 1998.

Clein, J. S., McGuire, A. D., Zhang, X., Kicklighter, D. W., Melillo, J. M., Wofsy, S. C., Jarvis, P. G., and Massheder, J. M.: Historical and projected carbon balance of mature black spruce ecosystems across north America: the role of carbon-nitrogen interaction, Plant Soil, 242, 15–32, 2002.

Dolman, A. J., Maximov, T. C., and Ohta, T.: Water and energy exchange in East Siberian forest: an introduction, Agr. Forest Meteorol., 148, 1913–1915, 2008.

Dolman, A. J., Maximov, T. C., Moors, E. J., Maximov, A. P., Elbers, J. A., Kononov, A. V., Waterloo, M. J., and van der Molen, M. K.: Net ecosystem exchange of carbon dioxide and water of far eastern Siberian Larch (*Larix cajanderii*) on permafrost, Biogeosciences, 1, 133–146, 2004, http://www.biogeosciences.net/1/133/2004/.

Engstrom, R., Hope, A., Kwon, H., Harazono, Y., Mano, M., and Oechel, W.: Modeling evapotranspiration in Arctic coastal plain ecosystems using a modified BIOME-BGC model, J. Geophys. Res., 111, G02021, doi:10.1029/2005JG000102, 2006.

Enting, I., Wigley, T., and Heimann, M.: Future emissions and concentrations of carbon dioxide: key ocean/atmosphere/land analyses. CSIRO Division of Atmospheric Research Technical Paper 31, 120 pp., 1994.

Euskirchen, E. S., McGuire, A. D., Kicklighter, D. W., Zhuang, Q., Clein, J. S., Dargaville,

Simulating larch forests

M. Ueyama et al.

⏮ | ⏭

◀ | ▶

Back | Close

Full Screen / Esc

R. J., Dye, D. G., Kimball, J. S., McDonald, K. C., Melillo, J. M., Romanovsky, V. E., and Smith, N. V.: Importance of recent shifts in soil thermal dynamics on growing season length, productivity, and carbon sequestration in terrestrial high-latitude ecosystems, Glob. Change Biol., 12, 731–750, 2006.

Farquhar, G. D., Von Caemmerer, S., and Berry, J. A.: A biochemical model of photosynthetic CO_2 assimilation in leaves of C_3 species, Planta, 149, 79–90, 1980.

Franks, S. W., Beven, K. J., Quinn, P. F., and Wright, I. R.: On the sensitivity of soil-vegetation-atmosphere transfer (SVAT) schemes: equifinality and the problem of robust calibration, Agr. Forest Meteorol., 86, 63–75, 1997.

Friedlingstein, P., Joel, G., Field, C. B., and fung, I. Y.: Towerd an allocation scheme for global terrestrial carbon models, Glob. Change Biol., 5, 755–770, 1999.

Gower, S. T. and Richards, J. H.: Larches: Deciduous conifers in an evergreen world, Bioscience, 40, 818–826, 1990.

Grant, R. F., Arain, A., Arora, V., Barr, A., Black, T. A., Chen, J., Wang, S., Yuan, F., and Zhang, Y.: Intercomparison of techniques to model high temperature effects on CO_2 and energy exchange in temperate and boreal coniferous forests, Ecol. Model., 188, 217–252, 2005.

Hinzman, L. D., Bettez, N. D., Bolton, W. R., Chapin, F. S., Dyurgerov, M. Fastie, C. L., Griffith, B., Hollister, R. D., Hope, A., Huntington, H. P., Jensen, A. M., Jia, G. J., Jorgenson, T., Kane, D. L., Klein, D. R., Kofinas, G., Lynch, A. H., Lloyd, A. H., McGuire, A. D., Nelson, F. E., Oechel, W. C., Osterkamp, T. E., Racine, C. H., Romanovsky, V. E., Stone, R. S., Stow, D. A., Sturm, M., Tweedie, C. E., Vourlitis, G. L., Walker, M. D., Waker, D. A., Webber, P. J., Welker, J. M., Winker, K. S., and Yoshikawa, K.: Evidence and implications of recent climate change in northern Alaska and other arctic regions, Climatic Change, 72, 251–298, 2005.

Hirano, T., Hirata, R., Fujinuma, Y., Saigusa, N., Yamamoto, S., Harazono, Y., Takeda, M., Inukai, K., and Inoue, G.: CO_2 and water vapor exchange of a larch forest in northern Japan, Tellus, 55B, 244–257, 2003.

Hirata, R., Hirano, T., Okada, K., Fujinuma, Y., Inukai, K., Saigusa, N., and Yamamoto, S.: Effect of wind speed and direction on eddy fluxes over a larch plantation, J. Agr. Meteorol., 60, 741–744, 2005.

Hirata, R., Hirano, T., Saigusa, N., Fujinuma, Y., Inukai, K., Kitamori, Y., Takahashi, Y., and Yamamoto, S.: Seasonal and interannual variations in carbon dioxide exchange of a temperate larch forest, Agr. Forest Meteorol., 147, 110–124, 2007.

Hirata, R., Saigusa, N., Yamamoto, S., Ohtani, Y., Ide, R., Asanuma, J., Gamo, M., Hirano,

Simulating larch forests

M. Ueyama et al.

T., Kondo, H., Kosugi, Y., Li, S.-G., Nakai, Y., Takagi, K., Tani, M., and Wang, H.: Spatial distribution of carbon balance in forest ecosystems across East Asia, Agr. Forest Meteorol., 148, 761–775, 2008.

Hollinger, D. Y., Kelliher, F. M., Schulze, E.-D., Bauer, G., Arneth, A., Byers, J. N., Hunt, J. E., McSeveny, T. M., Kobak, K. I., Milukova, I., Sogatchev, A., Tatarinov, F., Varlargin, A., Ziegler, W., and Vygodskaya, N. N.: Forest-atmosphere carbon dioxide exchange in eastern Siberia, Agr. Forest Meteorol., 90, 291–306, 1998.

IPCC: *IPCC (Intergovernmental Panel on Climate Change), Climate Change 2007*: Synthesis report Contribution of Working Groups I, II, and III to the Fourth Assessment Report of the Intergovernmental Panel on Climate Change, Cambridge University Press, Cambridge, UK, 104 pp, 2007.

Jarvis, P. G., Massheder, J. M., Hale, S. E., Moncrieff, J. B., Rayment, M., and Scott, S. L.: Seasonal variation of exchanges of a boreal black spruce forest, J. Geophys. Res., 102, 28953–28966, 1997.

Keyser, A.R., Kimball, J.S., Nemani, R. R., and Running, S. W.: Simulating the effects of climate change on the carbon balance of north American high-latitude forests, Glob. Change Biol., 6, 185–195, 2000.

Kajimoto, T., Matsuura, Y., Osawa, A., Prokushkin, A. S., Sofronov, M. A., and Abaimov, A. P.: Root system development of *Larix gmelinii* trees affected by micro-scale conditions of permafrost soils in central Siberia, Plant Soil, 255, 281–292, 2003.

Kajimoto, T., Matsuura, Y., Sofronov, M. A., Volokitina, A. V., Mori, S., Osawa, A., and Abaimov, A. P.: Above- and belowground biomass and net primary productivity of a *Larix gmelinii* stand near Tura, central Siberia, Tree Physiol., 19, 815–822, 1999.

Kim, H., Hirano, T., and Urano, S.: Seasonal variation in CO_2 production of leaf litter from different deciduous forest at the early decomposition stage, J. Agr. Meteorol., 61, 95–104, 2005.

Kimball, J. S., McDonald, K. C., Running, S. W., and Frolking, S. E.: Satellite radar remote sensing of seasonal growing seasons for boreal and subapline evergreen forests, Remote Sensing Environ., 90, 243–258, 2004.

Kimball, J. S., Thornton, P. E., White, M. A., and Running, S. W.: Simulating forest productivity and surface-atmosphere carbon exchange in the BOREAS study region, Tree Physiol., 17, 589–599, 1997a.

Kimball, J. S., White, M. A., and Running, S. W.: BIOME-BGC simulations of stand hydrologic

Simulating larch forests

M. Ueyama et al.

processes for BOREAS, J. Geophys. Res., 102, 29043–29051, 1997b.

Kimball, J. S., Zhao, M., McGuire, A. D., Heinsch, F. A., Clein, J., Calef, M., Jolly, W. M., Kang, S., Euskirchen, S. E., McDonald, K. C., and Running, S. W.: Recent climate-driven increases in vegetation productivity for the western arctic: evidence of an acceleration of the northern terrestrial carbon cycle, Earth Interact., 11, 1–30, 2007.

Kirdyanov, A., Houghes, M., Vaganov, E., Schweingruber, F., and Silkin, P.: The importance of early summer temperature and data of snow melt for tree growth in the Siberian Subarctic, Trees, 17, 61–69, 2003.

Kosugi, Y., Takanashi, S., Tanaka, H., Ohkubo, S., Tani, M., Yano, M., and Katayama, T.: Evapotranspiration over a Japanese cypress forest. I. Eddy covariance fluxes and surface conductance characteristics for 3 years, J. Hydrol., 337, 269–283, 2007.

Li, S.-G., Asanuma, J., Kotani, A., Eugster, W., Davaa, G., Oyunbaatar, D., and Sugita, M.: Year-round measurements of net ecosystem CO_2 flux over a montane larch forest in Mongolia, J. Geophys. Res., 110, D0930, doi:10.1029/2004JD005453, 2005.

Li, S.-G., Tsujimura, M., Sugimoto, A., Davaa, G., Oyunbaatar, D., and Sugita, M.: Temporal variation of $^{13}\delta C$ of larch leaves from a montane boreal forest in Mongolia, Trees, 21, 479–490, 2007.

Li, S. –G., Tsujimura, M., Sugimoto, A., Sasaki, L., Yamanaka, T., Davaa, G., Oyunbaatar, D., and Sugita, M.: Seasonal variation in oxygen isotope composition of waters for a montane larch forest in Mongolia, Trees, 20, 122–130, 2006.

Machimura, T., Iwahana, G., Lopez, L., Kobayashi, Y., Okabe, T., Yamada, Y., Hirano, T., Fukuda, M., and Fedorov, A. N.: Gross primary productivity, ecosystem respiration and net ecosystem exchange observed at a few intact and disturbed forests near Yakutsk, Eastern Siberia, Proceedings of International Workshop on: Tropical rain forest and boreal forest disturbance and their affects on global warming, 1–7, 2007.

Machimura, T., Kobayashi, Y., Iwahana, G., Hirano, T., Lopez, L., Fukuda, M. and Fedorov, A., N.: Change of carbon dioxide budget during three years after deforestation in eastern Siberian larch forest, J. Agr. Meteorol., 60, 653–656, 2005.

Manabe, S., Spelman, M. J., and Stouffer, R. J.: Transient responses of a coupled ocean-atmosphere model to gradual changes of atmospheric CO_2. part II: seasonal response, J. Climate, 5, 105–126, 1992.

Matyssek, R. and Schulze, E. –D.: Heterosis in hybrid larch (Larix deciduas x *leptolepis*), Trees, 225–231, 1987.

Simulating larch forests

M. Ueyama et al.

|◄ | ►|

◄ | ►

Back | Close

Full Screen / Esc

Printer-friendly Version

Interactive Discussion

Mizoguchi, Y., Miyata, A., Ohtani, Y., Hirata, R., and Yuta, S.: A review of tower observation sites in Asia, J. For. Res.-Jpn., 14, 1–9, 2009.

Myneni, R. B., Dong, J., Tucker, C. J., Kaufmann, R. K., Kauppi, P. E., Kauppi, P. E., Liski, J., Zhou, L., Alexeyev, V., and Hughes, M. K.: A large carbon sink in the woody biomass of northern forests, P. Natl. Acad. Sci. USA, 98, 14784–14789, 2001.

Nakai, Y., Matsuura, Y., Kajimoto, T., Abaimov, A. P., Yamamoto, S., and Zyryanova, O. A.: Eddy covariance CO_2 flux above a Gmelin larch forest on continuous permafrost in central Siberia during a growing season, Theor. Appl. Climatol., 93, 133–147, 2008.

Ohta, T., Hiyama, T., Tanaka, H., Kuwada, T., Maximov, T. C., Ohata, T., and Fukushima, Y.: Seasonal variation in the energy and water exchanges above and below a larch forest in eastern Siberia, Hydrol. Process, 15, 1459–1476, 2001.

Ohta, T., Maximov, T. C., Dolman, A. J., Nakai, T., van der Molen, M. K., Kononov, A. V., Maximov, A. P., Hiyama, T., Iijima, Y., Moors, E. J., Tanaka, H., Toba, T., and Yabuki, H.: Interannual variation of water balance and summer evapotranspiration in an eastern Siberian larch forest over a 7-year period (1998–2006), Agr. Forest Meteorol., 148, 1941–1953, 2008.

Piao, S., Ciais, P., Friedlingstein, P., Peylin, P., Reichstein, M., Luyssaert, S., Margolis, H., Fang, J., Barr, A., Chen, A., Grelle, A., Hollinger, D. Y., Laurila, T., Lindroth, A., Richardson, A. D., and Vesala, T.: Net carbon dioxide losses of northern ecosystems in response to autumn warming, Nature, 451, 49–53, 2007.

Pietsch, S. A., Hasenauer, H., and Thornton, P. E.,: BGC-model parameters for tree species growing in central European forests, Forest Ecol. and Manag., 211, 264–295, 2005.

Running, S. W. and Coughlan, J. C.: A general model of forest ecosystem processes for regional applications I. Hydrologic balance, canopy gas exchange and primary production processes, Ecol. Model., 42, 125–154, 1988.

Saigusa, N., Yamamoto, S., Hirata, R., Ohtani, Y., Ide, R., Asanuma, J., Gamo, M., Hirano, T., Kondo, H., Kosugi, Y., Li, S.-G., Nakai, Y., Takagi, K., Tani, M., and Wang, H.: Temporal and spatial variations in the seasonal patterns of CO_2 flux in boreal, temperate, and tropical forests in East Asia, Agr. Forest Meteorol., 148, 700–713, 2008.

Schulz, K., Jarvis, A., and Beven, K.: The predictive uncertainty of land surface fluxes in response to increasing ambient carbon dioxide, J. Climate, 14, 2551–2562, 2001.

Schulze, E. -D., Lloyd, J., Kelliher, F. M., Wirth, C., Rebmann, C., Luhker, B., Mund, M., Knohl, A., Milyukova, I. M., Schulze, W., Ziegler, W., Varlagin, A. β., Sogachev, A. F., Valentini, R., Dore, S., Grigoriev, S., Kolle, O., Panfyorov, M. I., Tchebakova, N., and Vygodskaya, N. N.:

Productivity of forests in the Eurosiberian boreal region and their potential to act as a carbon sink – a synthesis, Glob. Change Biol., 5, 703–722, 1999.

Sitch, S., Smith, B., Prentice, I. C., Arneth, A., Bondeau, A., Cramer, W., Kaplan, J. O., Levis, S., Lucht, W., Sykes, M. T., Thonicke, K., and Venevsky, S.: Evaluation of ecosystem dynamics, plant geography and terrestrial carbon cycleing in the LPJ dynamic global vegetation model, Glob. Change Biol., 9, 161–185, 2003.

Tans, P. P., and Conway, T. J.: Monthly atmospheric CO_2 mixing ratios from the NOAA CMDL carbon cycle cooperative global air sampling network, 1968-2002, In Trends: A compendium of data on global change. carbon dioxide information analysis center, Oak Ridge National Laboratory, US Department of Energy, Oak Ridge, Tenn., USA, 2005.

Turner, D. P., Ritts, W. D., Cohen, W. B., Gower, S. T., Zhao, M., Running, S. W., Wofsy, S. C., Urbanski, S., Dunn, A. L., and Munger, J. W.: Scaling gross primary production (GPP) over boreal and deciduous forest landscapes in support of MODIS GPP product validation, Remote Sensing Environ., 88, 256–270, 2003.

Thornton, P. E., Law, B. E., Gholz, H. L., Clark, K. L., Falge, E., Ellsworth, D. S., Goldstein, A. H., Monson, R. K., Hollinger, D., Falk, M., Chen, J., and Sparks, J. P.: Modeling and measuring the effects of disturbance history and climate on carbon and water budgets in evergreen needle forests, Agr. Forest Meteorol., 113, 185–222, 2002.

Ueyama, M., Harazono, Y., Kim, Y., and Tanaka, N.: Response of the carbon cycle in sub-arctic black spruce forests to climate change; reduction of a carbon sink related to the sensitivity of heterotrophic respiration, Agr. Forest Meteorol., 149, 582–602, 2009.

Vaganov, E. A., Hughes, M. K., Kirdyanov, A. V., Schweingruber, F. H., and Silkin, P. P.: Influence of snowfall and melt timing on tree growth in subarctic Eurasia, Nature, 400, 149–151, 1999.

Valentini, R., Matteucci, G., Dolman, A. J., Schulze, E. -D., Rebmann, C., Moors, E. J., Granier, A., Gross, P., Jensen, N. O., Pilegaard, K., Lindroth, A., Grelle, A., Bernhofer, C., Grûnwald, T., Aubinet, M., Ceulemans, R., Kowalski, A.S., Vesala, T., Rannik, ., Berbigier, P., Loustau, D., Guδmundsson, J., Thorgeirsson, H., Lbrom,A. Morgenstern, K., Clement, R., Moncrieff, J., Montagnani, L., Minerbi, S., and Jarvis, P. G.: Respiration as the main determinant of carbon balance in European forests, Nature, 404, 861–865, 2000.

Vogel, J., Bond-Lamberty, B. P., Schuur, E. A. G., Gower, S., Mack, M. C., O'Connell, K. B. O., Valentine, D. W., and Ruess, R. W.: Carbon allocation in boreal black spruce forests across regions varying in soil temperature and precipitation, Glob. Change Biol., 14, 1503–1516,

Simulating larch forests

M. Ueyama et al.

◄ | ►|

◄ | ►

Back | Close

Full Screen / Esc

Printer-friendly Version

Interactive Discussion

2008.

Vygodskaya, N. N., Milyukova, I., Varlagin, A., Tatarinov, F., Sogachev, A., Kobak, K. I., Desyatkin, R., Bauer, G., Hollinger, D. Y., Kelliher, F. M., and Schulze, E.-D.: Leaf conductance and CO_2 assimilation of *Larix gmelinii* growing in an eastern Siberian boreal forest, Tree Physiol., 17, 607–615, 1997.

Wang, H. Zu, Y., Saigusa, N., Yamamoto, S., Kondo, H., Yang, F., and Wang, W.: CO_2, water vapor and energy fluxes in a larch forest in northeast China, J. Agr. Meteorol., 60, 549–552, 2005a.

Wang, H., Saigusa, N., Zu, Y., Yamamoto, S., Kondo, H., Yang, F., Wang, W., Hirano, T., and Fujinuma, Y.: Response of CO_2 flux to environmental variables in two larch forest ecosystems in east Asia, Phyton-Ann. Rei. Bot. A, 45, 339–346, 2005b.

Webb, R. S., Rosenzweig, C. E., and Levine, E.R.: Specifying land surface characteristics in general circulation models: soil profile data set and derived water-holding capacities, Global Biogeochem. Cy., 7, 97–108, 1993.

Welp, L. R., Randerson, J. T., and Liu, H. P.: The sensitivity of carbon fluxes to spring warming and summer drought depends on plant functional type in boreal forest ecosystems, Agr. Forest Meteorol., 147, 172–185, 2007.

White, M. A., Thornton, P. E., Running, S. W., and Nemani, R. R.: Parameterization and sensitivity analysis of the BIOME-BGC terrestrial ecosystem model: Net primary production controls, Earth Interact., 4, 1–85, 2000.

Wilson, K. B., Baldocchi, D. D., and Hanson, P. J.: Spatial and seasonal variability of photosynthetic parameters and their relationship to leaf nitrogen in a deciduous forest, Tree Physiol., 20, 565–578, 2000.

Wilson, K., Goldstein, A., Falge, E., Aubinet, M., Baldocchi, D., Berbigier, P., Bernhofer, C., Ceulemans, R., Dolman, H., Field, C., Grelle, A., Ibrom, A., Law, B. E., Kowalski, A., Meyers, T., Moncrieff, J., Monson, R., Oechel, W., Tenhunen, J., Valentini, R., and Verma, S.: Energy balance closure at FLUXNET sites, Agr. Forest Meteorol., 113, 223–243, 2002.

Zhang, Y., Rossow, W., Lacis, A. A., Oinas, V., and Mishchenko, M.: Calculation of radiative fluxes from the surface to top of atmosphere based on ISCCP and other global data sets: refinements of the radiative transfer model and the input data, J. Geophys. Res., 112, D19105, doi:10.1029/2003JD004457, 2004.

Zober, L.: A World Soil File for Global Climate Modeling, NASA Technical Memorandum 87802, NASA, 33 pp., 1986.

Simulating larch forests

M. Ueyama et al.

Printer-friendly Version

Interactive Discussion

Table 1. Site characteristics.

Site	Latitude	Longitude	Elevation (m)	Species	LAI[a]	Stand age	Stand height	year
TMK	42°44′ N	141°31′ E	140	*Larix kaempferi*	9.2 (5.6)	45	15	2001–2003
LSH	45°20′ N	127°34′ E	370	*Larix gmelinii*	(2.5)	34	17	2004
SKT	48°21′ N	108°39′ E	1630	*Larix sibirica*	4.4 (2.7)	70~150	20	2003–2005
YLF	62°15′ N	129~14′ E	220	*Larix cajanderii*	3.7 (1.6)	160	18	2004
NEL	62°19′ N	129°14′ E	200	*Larix cajanderii*	2.9 (1.9)	N/A	21	2003–2005
TUR	642°16′ N	100°12′ E	250	*Larix gmelinii*	(0.3)	105	3.4	2004

[a] Total LAI (larch LAI)

Table 2. Parameters used in the BIOME-BGC model.

Parameter	Original	Modified
annual leaf and fine root turnover fraction (yr^{-1})	1.00	
annual live wood turnover fraction (yr^{-1})	0.70	
annual whole-plant mortality fraction (yr^{-1})	0.005	
annual fire mortality fraction (yr^{-1})	0.005	
new fine root C : new leaf C	1.4	--[a]
new stem C : new leaf C	2.2	0.31[b]
new live wood C : new total wood C	0.071	
new coarse root C : new stem C	0.29	0.56[b]
current growth proportion	0.5	
C:N of leaves (kg C kg N^{-1})	27	
C:N of leaf litter, after retranslocation (kg C kg N^{-1})	120	
C:N of fine roots (kg C kg N^{-1})	58	
C:N of live wood (kg C kg N^{-1})	50	
C:N of dead wood (kg C kg N^{-1})	730	
leaf litter labile proportion	0.31	
leaf litter cellulose proportion	0.45	
leaf litter lignin proportion	0.24	
fine root labile proportion	0.34	
fine root cellulose proportion	0.44	
fine root lignin proportion	0.22	
dead wood lignin/cellulose proportion	0.29/0.71	
canopy water interception coefficient (LAI^{-1} d^{-1})	0.045	0.045 (0.005)[c]
canopy light extinction coefficient (m^2 kg C^{-1})	0.51	
all-sided to projected leaf area ratio	2.6	
canopy average specific leaf area	22.0	16.0[d]
ratio of shaded SLA:sunlit SLA*	2.0	
fraction of leaf N in Rubisco	0.088	0.050[e]
maximum stomatal conductance (m s^{-1})	0.006	0.003[f]
cuticular conductance (m s^{-1})	0.00006	
boundary layer conductance (m s^{-1})	0.09	
PSI*: start of conductance reduction (MPa)	−0.63	−0.70[g]
PSI*: start of conductance reduction (MPa)	−2.30	−2.60[g]
VPD: complete conductance reduction (Pa)	610	800[g]
VPD: complete conductance reduction (Pa)	3100	3200[g]

* PSI, leaf and soil water potential
* SLA, specific leaf area
[a] Determined each site.
[b] Kajimoto et al. (1999)
[c] 0.045 for the sites of TMK, SKT, YLF, NEL, and TUR, whereas 0.005 for LSH.
[d] Matyssek and Schulze (1987)
[e] ranged in previous examined values: Pitsch et al. (1991), and Vygodskaya et al. (1997)
[f] Turner et al. (2003)
[g] Pietsch et al. (1991)

Simulating larch forests

M. Ueyama et al.

Title Page

Abstract | Introduction

Conclusions | References

Tables | Figures

|◄ | ►|

◄ | ►

Back | Close

Full Screen / Esc

Printer-friendly Version

Interactive Discussion

Table 3. Climate biases applied into the sensitivity study. The bias for each season was determined as three times the standard deviation of the natural variability from the long-term climate data shown in Fig. 1.

		TMK	LSH	SKT	YLF	TUR
Air Temperature (^{o}C)	spring	2.8	3.7	6.0	5.1	6.0
	summer	2.9	2.1	5.1	3.0	3.4
	autumn	2.2	2.8	5.2	5.3	6.9
	winter	3.2	5.1	7.7	8.1	10.2
Precipitation (%)	spring	53	54	54	59	61
	summer	53	39	47	57	57
	autumn	62	53	42	53	57
	winter	57	63	82	60	55
VPD (%)	spring	58	41	43	43	42
	summer	54	45	49	39	46
	autumn	22	38	44	39	48
	winter	40	69	38	69	33
Solar Radiation (%)	spring	13	7	6	6	8
	summer	22	10	7	8	9
	autumn	14	8	18	15	20
	winter	19	6	30	24	41

Table 4. Root mean square error (RMSE) between observed and simulated carbon and water fluxes at a daily time scale.

Site		NEE $\mathrm{g\,C\,m^{-2}\,d^{-1}}$	GPP $\mathrm{g\,C\,m^{-2}\,d^{-1}}$	RE $\mathrm{g\,C\,m^{-2}\,d^{-1}}$	ET $\mathrm{mm\,d^{-1}}$
TMK	original	1.6	2.6	2.4	2.0
	improved	1.4	1.5	1.2	3.0
LSH	original	2.2	2.5	1.3	2.1
	improved	1.3	1.3	1.0	1.0
SKT	original	0.9	1.1	0.5	0.8
	improved	0.9	1.1	0.8	0.8
YLF	original	1.5	3.2	1.9	1.0
	improved	1.3	1.5	0.7	0.7
NEL	original	1.6	1.6	1.6	1.6
	improved	1.4	1.5	1.6	1.6
TUR	original	0.9	2.0	1.6	0.9
	improved	0.7	0.7	0.6	0.9
average	original	1.5	2.3	1.5	1.3
	improved	1.2	1.3	1.0	1.2

Table 5. The sensitivity of annual GPP, RE, and NEE to changes in weather patterns of temperature, precipitation, VPD, and solar radiation. The numbers in the table are the relative percentage as compared to the control experiment. The applied climate bias in each season was determined as 3 of the natural variability (Table 3). The underscores in the table represent the values that show a high sensitivity for changing GPP and RE (more than 10%) and NEE (more than 20%) compared to the control experiment.

Examination	Case	GPP (%)						RE (%)						NEE (%)					
		TMK	LSH	SKT	YLF	NEL	TUR	TMK	LSH	SKT	YLF	NEL	TUR	TMK	LSH	SKT	YLF	NEL	TUR
	Normal	100	100	100	100	100	100	100	100	100	100	100	100	100	100	100	100	100	100
Air temperature	spring +	113	109	110	106	109	119	109	108	112	105	102	115	142	136	99	111	224	158
	spring −	87	91	99	96	95	92	91	93	98	97	112	91	53	59	105	89	−179	100
	summer +	98	102	110	107	111	115	104	106	123	117	112	121	42	45	46	44	90	67
	summer −	100	98	80	87	87	82	95	94	80	84	90	81	144	146	77	105	37	91
	autumn +	100	101	107	103	109	110	103	105	110	110	108	119	73	56	91	59	128	−22
	autumn −	99	98	95	95	93	91	97	96	96	93	97	88	123	126	90	104	35	119
	winter +	98	100	100	99	102	101	100	102	105	104	104	106	81	62	75	63	73	61
	winter −	102	100	100	101	98	100	100	98	97	96	96	96	125	135	114	128	123	140
Precipitation	spring +	100	100	107	103	108	100	100	100	104	107	104	100	99	99	121	72	24	100
	spring −	100	99	89	96	94	100	100	99	96	94	91	100	99	105	58	111	134	100
	summer +	100	100	122	104	115	100	100	101	126	108	132	101	97	95	101	80	−136	97
	summer −	100	99	67	90	89	99	100	98	82	94	85	97	97	117	−9	63	140	126
	autumn +	100	100	103	100	107	100	100	101	103	100	115	100	100	98	86	102	100	−5
	autumn −	100	100	97	100	92	100	99	99	97	100	89	100	109	118	95	100	140	101
	winter +	100	100	100	101	104	100	100	100	100	102	107	100	101	100	101	94	63	100
	winter -	100	100	100	99	96	100	100	100	100	98	94	100	100	100	99	105	122	100
VPD	spring +	100	99	98	100	98	100	100	100	99	100	98	100	100	92	93	101	109	100
	spring −	100	100	102	100	102	100	100	100	101	100	103	100	99	102	109	99	83	100
	summer +	99	92	83	88	92	98	99	98	93	97	101	99	104	−1	38	28	−30	90
	summer −	100	102	122	110	112	101	100	101	118	111	120	101	97	114	145	105	3	101
	autumn +	100	100	98	99	99	100	100	99	98	100	98	100	100	104	96	97	108	100
	autumn −	100	100	103	101	102	100	100	101	104	100	103	100	99	87	101	102	81	100
	winter +	100	100	100	100	100	100	100	100	100	100	100	100	100	100	100	100	100	100
	winter −	100	100	100	100	100	100	100	100	100	100	100	100	100	100	100	100	100	100
Solar Radiation	spring +	101	100	100	100	100	100	100	100	100	100	100	100	104	103	99	100	102	100
	spring −	99	100	100	100	100	100	99	100	100	100	100	100	93	97	101	100	98	100
	summer +	112	102	100	102	100	102	106	100	99	99	97	100	170	124	100	118	136	118
	summer −	86	98	101	97	100	98	93	100	101	101	103	100	22	70	100	76	50	79
	autumn +	103	101	100	100	100	100	101	100	100	100	100	100	117	111	101	102	108	103
	autumn −	97	99	100	100	99	99	99	100	100	100	101	100	83	88	99	98	89	95
	winter +	100	100	100	100	100	100	100	100	100	100	100	100	100	100	100	100	100	100
	winter −	100	100	100	100	100	100	100	100	100	100	100	100	100	100	100	100	100	100

Title Page

Abstract Introduction

Conclusions References

Tables Figures

◄ ►

◄ ►

Back Close

Full Screen / Esc

Printer-friendly Version

Interactive Discussion

Fig. 1. Location of study sites from northern Eurasia to East Asia. The gray area represents a distribution of larch forest based on the MOD12 landcover classification.

Simulating larch forests

M. Ueyama et al.

Title Page

Abstract	Introduction
Conclusions	References
Tables	Figures

|◄ | ►|

◄ | ►

Back | Close

Full Screen / Esc

Printer-friendly Version

Interactive Discussion
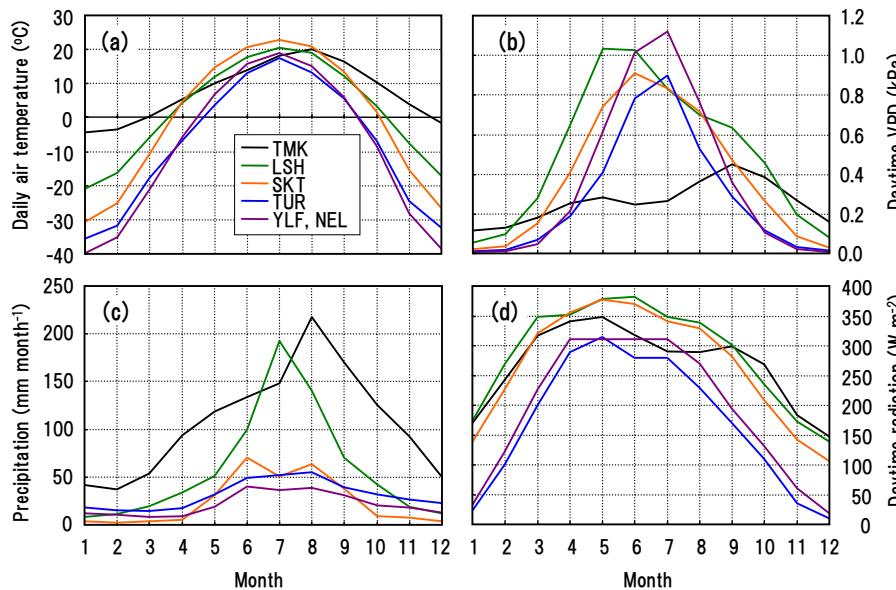
Fig. 2. Seasonal variations of climate variables: **(a)** air temperature, **(b)** daytime VPD, **(c)** precipitation, and **(d)** daytime solar radiation. The data are derived from weather stations near the site from 1961 to 2000, except that the daytime solar radiation are from the International Satellite Cloud Climatology Project Radiation Flux Profile data (Zhang et al., 2004) from 1984 to 2000. The climate data of TMK are from the Japan Meteorological Agency, and those of other sites are from the National Climate Data Center.
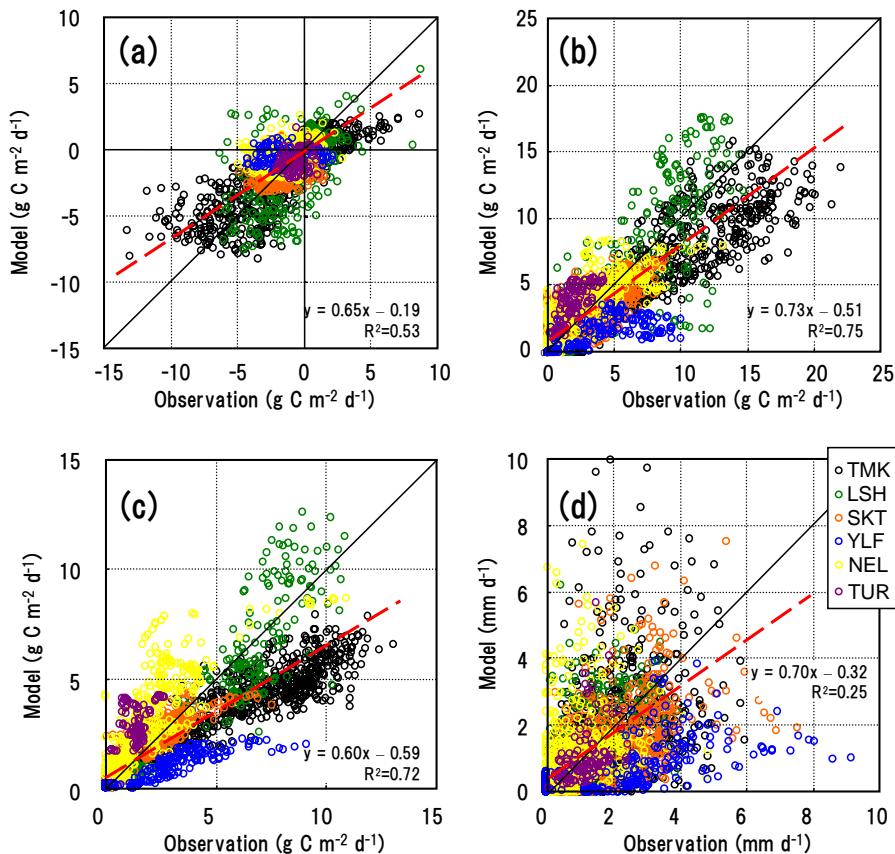
Fig. 3. Observed and modeled (original BIOME-BGC) daily **(a)** NEE, **(b)** GPP, **(c)** RE, and **(d)** ET. Solid and dashed lines represent the 1:1 and regression lines, respectively.
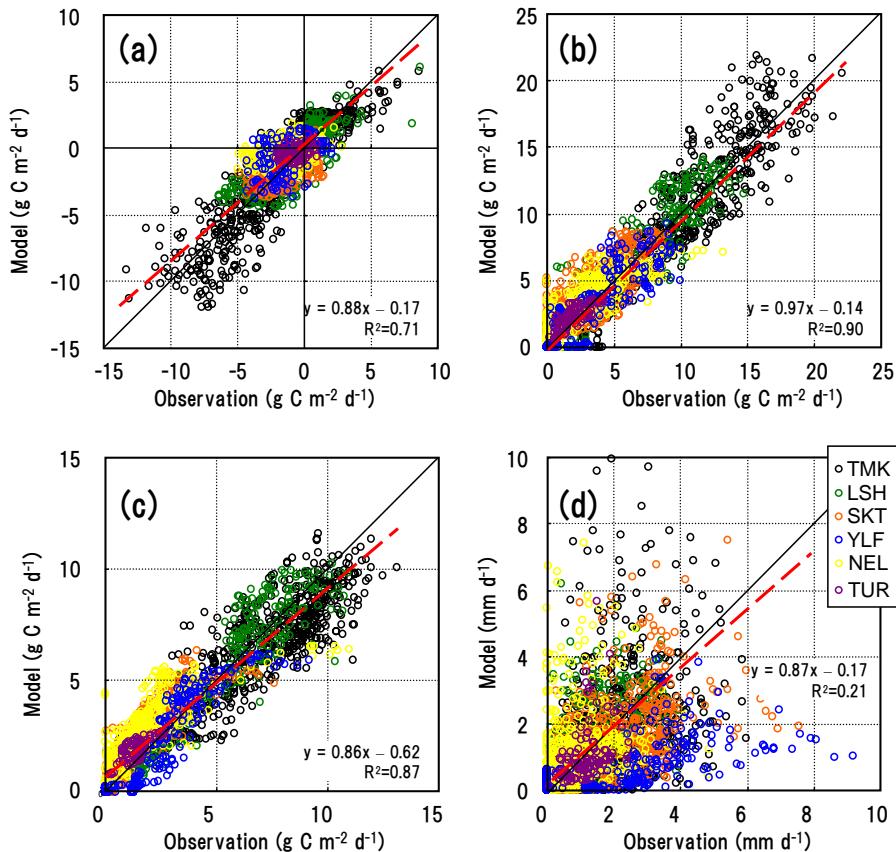
Fig. 4. Observed and modeled (improved BIOME-BGC) daily **(a)** NEE, **(b)** GPP, **(c)** RE, and **(d)** ET. Solid and dashed lines represent the 1:1 and regression lines, respectively.
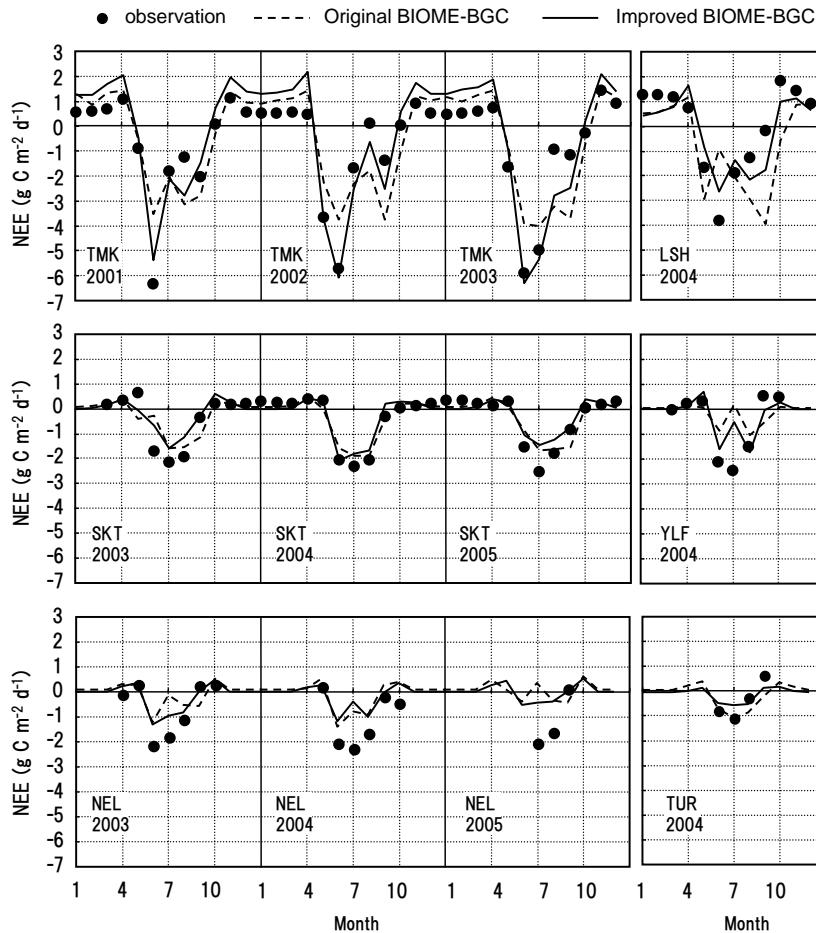
Fig. 5a. Monthly variations of observed (black dots) and simulated (solid lines for the improved model and dashed lines for the original model) **(a)** NEE, **(b)** GPP, **(c)** RE, and **(d)** ET.
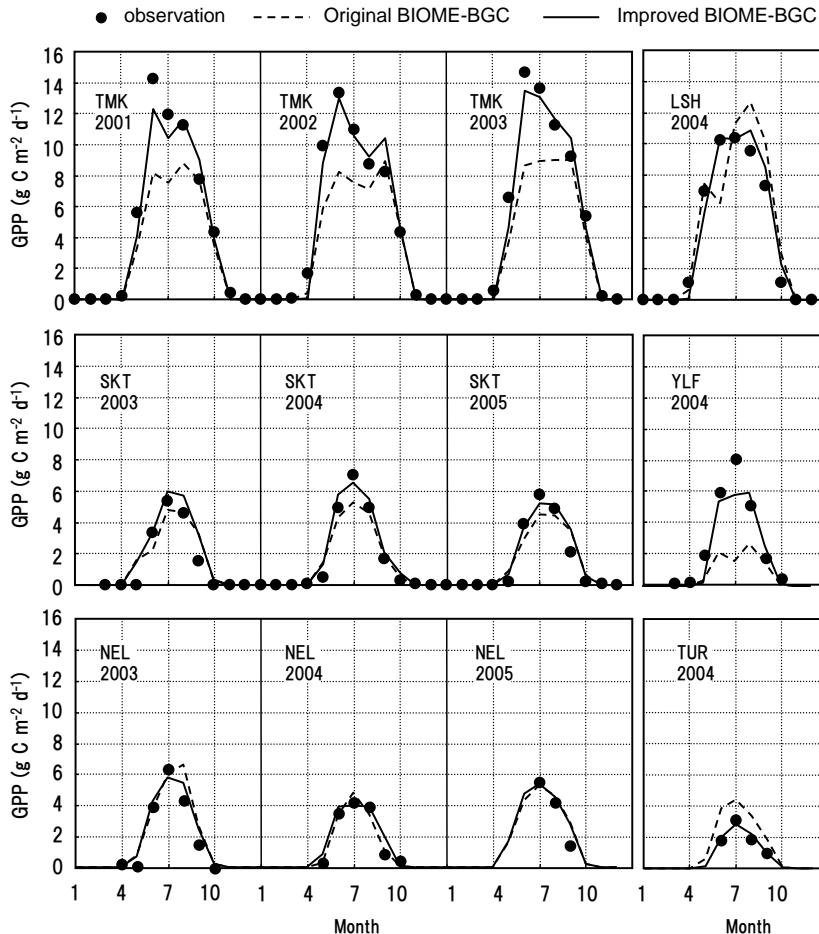
Fig. 5b. Continued.

Fig. 5c. Continued.

Fig. 5d. Continued.

Back | Close

Full Screen / Esc

Printer-friendly Version

Interactive Discussion
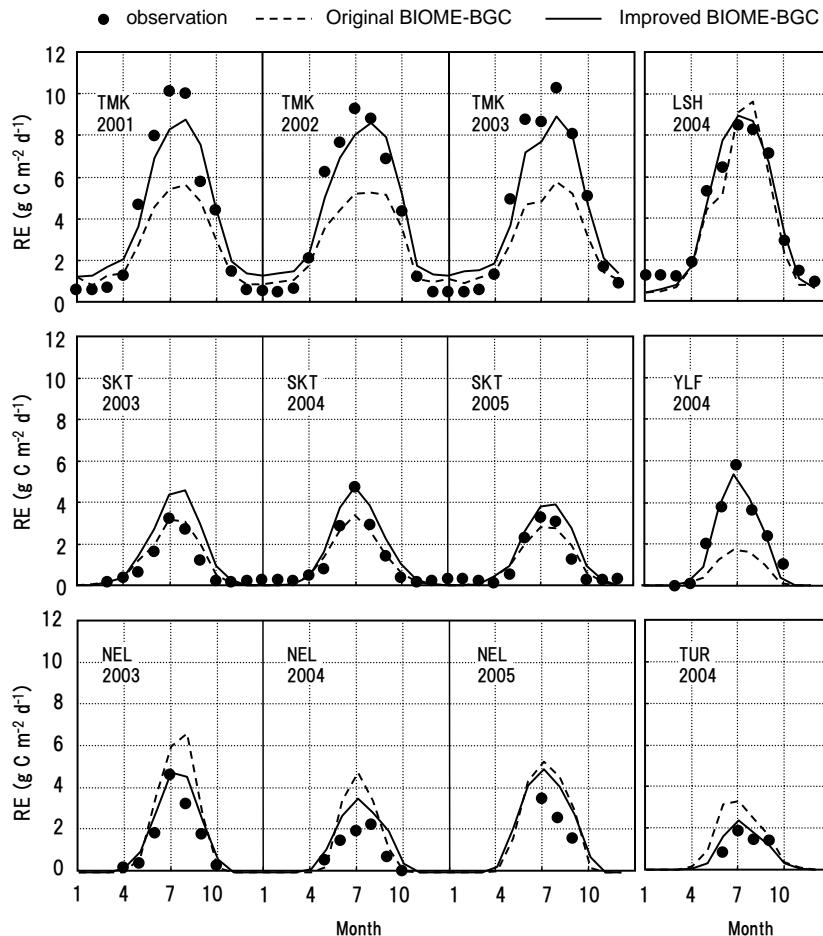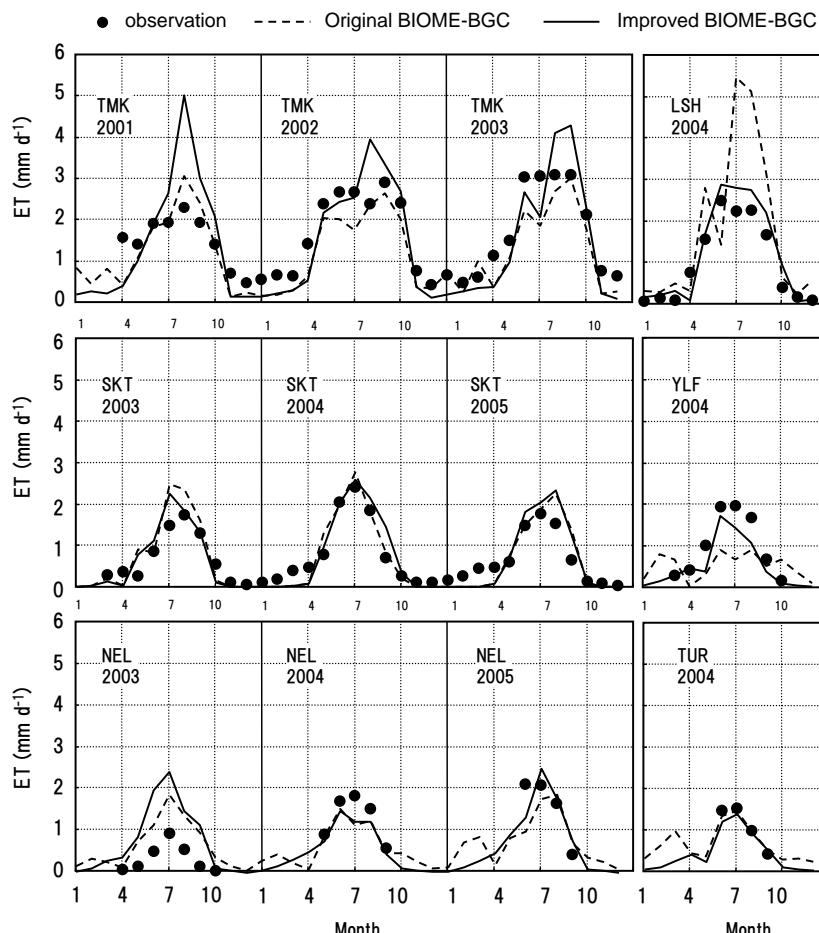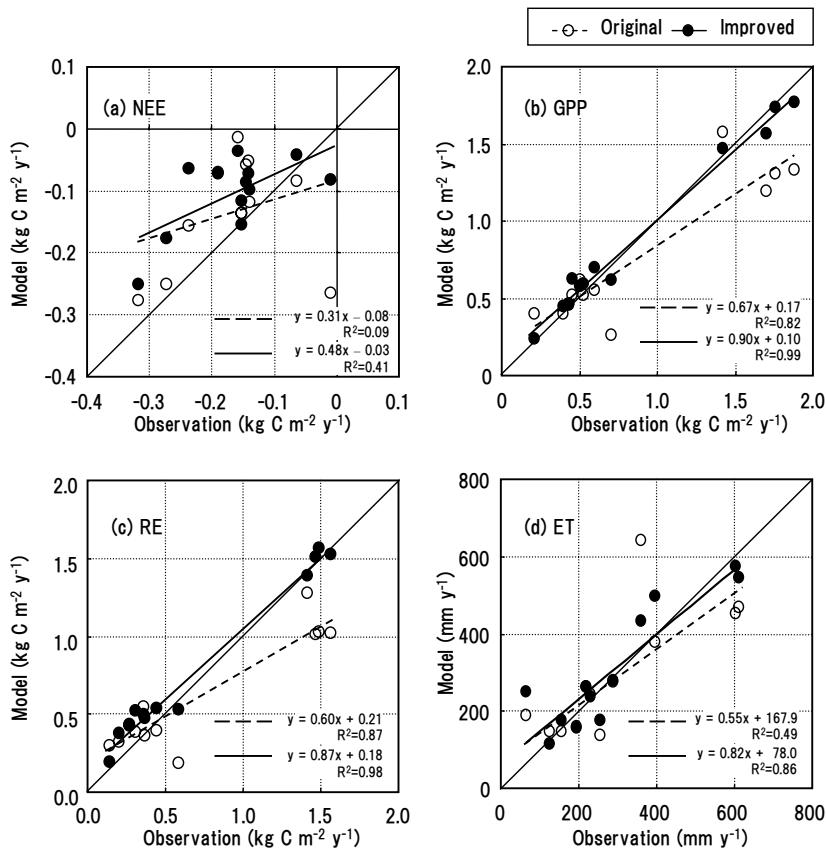
Fig. 6. Observed and modeled (white dots for the original model and black dots for the improved model) **(a)** NEE, **(b)** GPP, **(c)** RE, and **(d)** ET at an annual time scale. Regression lines (dashed line for the original model and solid line for the improved model) are also shown.
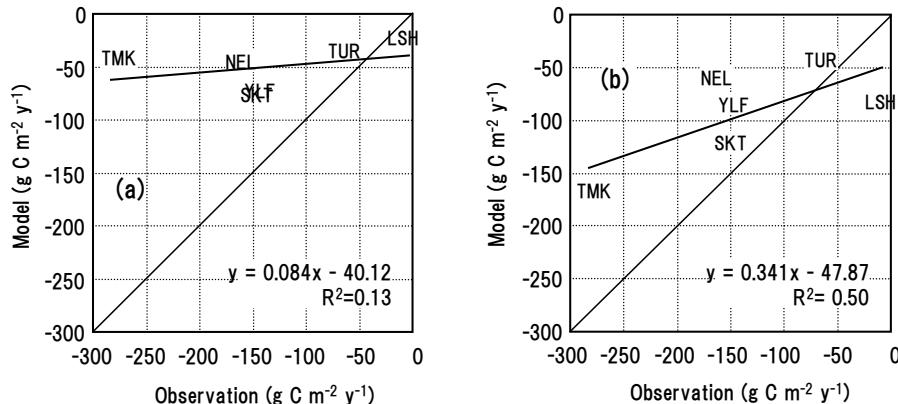
Fig. 7. Observed and simulated annual NEE **(a)** without and **(b)** with stand history. The annual values were only calculated during the period when observed data were available.
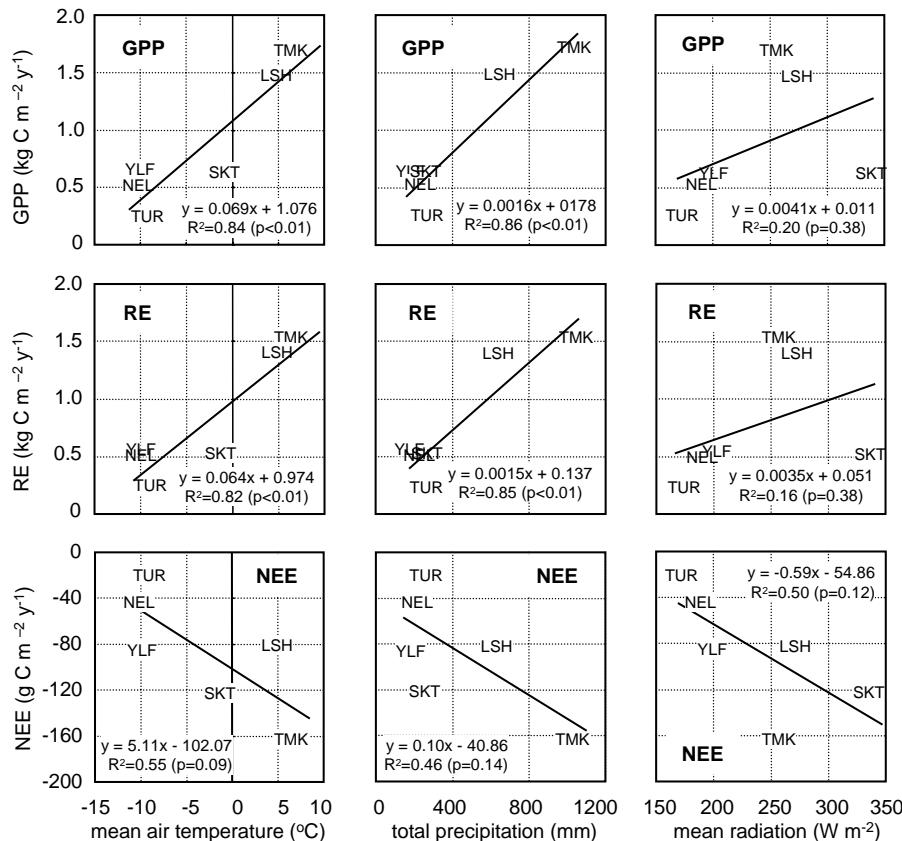
Fig. 8. Relationships between mean annual climate variables (air temperature, precipitation, and radiation) and simulated annual GPP, RE, and NEE. Symbols are as in Table 1.

Title Page

Abstract | Introduction

Conclusions | References

Tables | Figures

|◄ | ►|

◄ | ►

Back | Close

Full Screen / Esc

Printer-friendly Version

Interactive Discussion
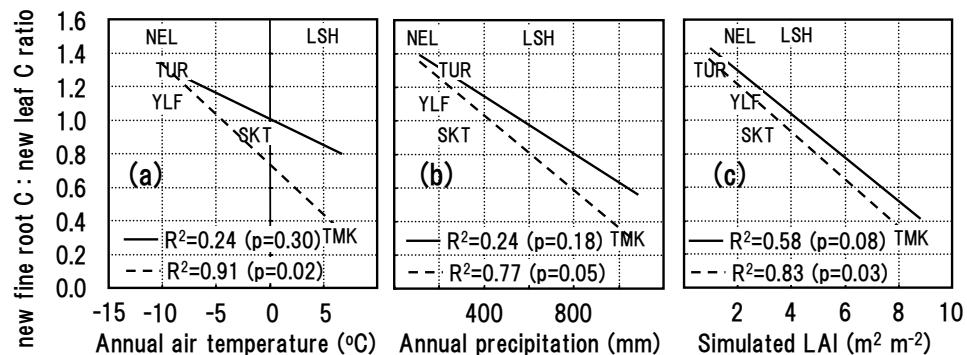
Fig. 9. Relationships between the allocation ratio of new fine root C to new leaf C and **(a)** mean annual air temperature, **(b)** total annual precipitation, and **(c)** LAI simulated by the improved model. Solid lines are derived from all sites, whereas dashed lines are from all sites except LSH.